Accuracy of magnetic resonance imaging for measuring maturing cartilage: A phantom study

Jennifer R. McKinney,[I] Marshall S. Sussman,[II] Rahim Moineddin,[III] Afsaneh Amirabadi,[I] Tammy Rayner,[I] Andrea S. Doria[I,II,*]

[I] University of Toronto, The Hospital for Sick Children, Department of Diagnostic Imaging, Toronto/ON, Canada. [II] The University Health Network, Toronto General Hospital, Department of Medical Imaging, Toronto/ON, Canada. [III] University of Toronto, Department of Family and Community Medicine, Toronto/ON, Canada.

OBJECTIVES: To evaluate the accuracy of magnetic resonance imaging measurements of cartilage tissue-mimicking phantoms and to determine a combination of magnetic resonance imaging parameters to optimize accuracy while minimizing scan time.

METHOD: Edge dimensions from 4 rectangular agar phantoms ranging from 10.5 to 14.5 mm in length and 1.25 to 5.5 mm in width were independently measured by two readers using a steel ruler. Coronal T1 spin echo (T1 SE), fast spoiled gradient-recalled echo (FSPGR) and multiplanar gradient-recalled echo (GRE MPGR) sequences were used to obtain phantom images on a 1.5-T scanner.

RESULTS: Inter- and intra-reader reliability were high for both direct measurements and for magnetic resonance imaging measurements of phantoms. Statistically significant differences were noted between the mean direct measurements and the mean magnetic resonance imaging measurements for phantom 1 when using a GRE MPGR sequence (512x512 pixels, 1.5-mm slice thickness, 5:49 min scan time), while borderline differences were noted for T1 SE sequences with the following parameters: 320x320 pixels, 1.5-mm slice thickness, 6:11 min scan time; 320x320 pixels, 4-mm slice thickness, 6:11 min scan time; and 512x512 pixels, 1.5-mm slice thickness, 9:48 min scan time. Borderline differences were also noted when using a FSPGR sequence with 512x512 pixels, a 1.5-mm slice thickness and a 3:36 min scan time.

CONCLUSIONS: FSPGR sequences, regardless of the magnetic resonance imaging parameter combination used, provided accurate measurements. The GRE MPGR sequence using 512x512 pixels, a 1.5-mm slice thickness and a 5:49 min scan time and, to a lesser degree, all tested T1 SE sequences produced suboptimal accuracy when measuring the widest phantom.

KEYWORDS: Cartilage; Dimensional Measurement Accuracy; Magnetic Resonance Imaging; Pediatrics; Phantoms.

◼ INTRODUCTION

Magnetic resonance imaging (MRI) is a non-invasive, multiplanar imaging modality that enables three-dimensional assessments of joints and their surrounding soft tissue structures. MRI is the method of choice for the direct, non-invasive visualization of cartilage (1). MRI-derived cartilage measurements are useful for exploring the effects of modifiable risk factors on articular cartilage prior to clinical disease and for identifying potential preventive strategies. Thus, these measurements are of great value for monitoring treatment responses in childhood arthritis (2-4). However, the small dimensions of pediatric articular cartilage make the measurement of this tissue using conventional MRI scanners challenging, as such, it is difficult to obtain accuracy in such measurements. While past studies have established that MRI-derived cartilage measurements produce high face validity when using cadaveric and surgical specimens from adults (5-12), to our knowledge, few if any prior studies have determined the criterion validity of MRI-based measurements of maturing cartilage using cadaveric or surgical specimens or phantoms as reference standards. Currently, most of the available information in the literature relates to observational studies the effects of sex, age, growth, Tanner stage and physical activity on articular cartilage volume (12,13).

Determining the accuracies of different MRI sequences currently being used in clinical practice to assess maturing cartilage in children and adolescents is crucial given that articular cartilage thickness tends to reduce during physiologic

growth. Therefore, accurate measurements are required to discriminate minimal arthropathy (which requires treatment) from normal physiologic growth. The goals of the current study were to assess the inter- and intra-reader reliabilities of direct and MRI-acquired measurements of phantoms, to evaluate the accuracies of MRI-derived measurements of pediatric articular cartilage using four different-sized agar phantoms designed to mimic the average dimensions of pediatric cartilage tissue and to determine the combination of MRI sequences and parameters that optimizes accuracy while minimizing scan time.

■ MATERIALS AND METHODS

Phantom Preparation and Measurements

Four rectangular tissue-mimicking phantoms composed of distilled water and 3% by mass agar (high-strength A-6924 Sigma Chemical, St Louis, MO) were prepared as described elsewhere (14) and served as pediatric cartilage samples (Figure 1a). The phantoms consisted of four variably sized agar-based prototypes that were customized to encompass orthogonally intersecting walls with top-view edge dimensions in length x width of 14.4 x 5.5 mm (phantom 1), 13.6 x 3.8 mm (phantom 2), 10.6 x 2.1 mm (phantom 3) and 14.6 x 1.3 mm (phantom 4). The phantoms' edge dimensions were independently measured by two readers, a pediatric radiologist (A.S.D.) and a clinical research assistant (J.R.M.), using a 15-cm calibrated steel ruler. The dimensions were measured twice by the readers, who were blinded to each other's results. All dimensions were recorded in mm. These direct measurements served as the reference standards for this study.

MRI Protocol and Interpretation

Imaging was conducted on a 1.5 Tesla Twin Speed MRI scanner (General [GE] Electric Medical Systems, Milwaukee, WI, USA) using an 8-channel volumetric knee coil. Coronal T1-weighted spin-echo (T1 SE) [3 sequences with different parameters], fast spoiled gradient-recalled echo (FSPGR) [3 sequences with different parameters] and multiplanar gradient-recalled echo (GRE MPGR) [2 sequences with different parameters] images of the phantoms were obtained while they were embedded in a saline-Magnevist® bath at a concentration of 469 mg/mL [0.5 mmol/mL]) (Figure 1b). Details on the MRI sequences are available in Table 1. The MR images (Figure 2) were independently viewed and measured on a General Electric (GE) Advantage Workstation (software version 4.2, General Electric Medical Systems) by the readers. The MRI data were read twice by each reader in a random order. A two-week interval was used between baseline and repeat measurements to reduce any potential recall effect. The readers were blinded to each other's measurements as well as to their own baseline sets of measurements.

Signal-to-Noise Ratio Calculation

Signal-to-noise ratios (SNRs) were obtained for the MR images of the phantoms using each sequence, as outlined in Table 1. Using the GE Advantage Workstation, three small circular regions of interest (ROIs) (area = 1 mm^2) were positioned within each phantom (Figure 3). Due to the small size and shape variations of the phantoms, one large ROI could not be used. The signal intensity (SI, defined as the mean pixel intensity value in a ROI) was recorded for each ROI (three ROIs per phantom) and averaged to yield the mean SI for each phantom. The noise was defined as the standard deviation (SD) in pixel intensity from three small circular ROIs placed in background air (homogeneous area, free from ghosting artifacts) (15). The SNR was calculated as SNR=0.65*(SI/SD), employing a correction factor of 0.65 for background noise (Rician distribution) (16).

Spatial Resolution

Spatial resolution served as a factor in determining the accuracy of an MRI sequence for measuring maturing cartilage and was calculated as spatial resolution (gross assessment) = field of view/matrix (17).
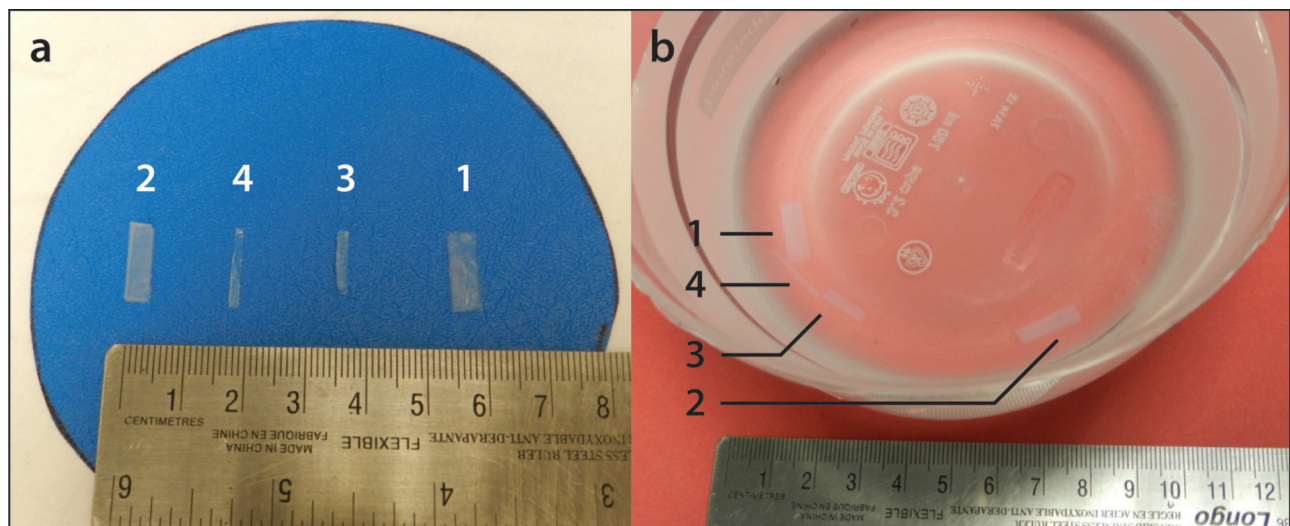
Figure 1 - Layout of cartilage-mimicking phantoms (1-4) on a planar surface in ambient air (a) and embedded in a saline-Magnevist® bath (b).

Table 1 - Magnetic resonance imaging sequence parameters and statistically significant differences (*p*-values) between the mean direct measurements and the mean MRI measurements (shown in bold).

	Pulse sequence	T1 SE			GRE MPGR		FSPGR		
MRI parameters	Matrix (pixels)	320x320	320x320	512x512	320x320	512x512	512x512	512x512	1024x1024
	Slice thickness (mm)	1.5	4	1.5	4	1.5	1.5	0.5	1.5
	NEX	2	2	2	2	2	1	1	1
	Scan time (min)	6:11	6:11	9:48	3:40	5:49	3:36	3:38	10:33
	TE (ms)	12	12	12	15	15	Min full	Min full	Min full
	TR (ms)	568	568	568	450	450	N/A	N/A	N/A
	Bandwidth (kHz)	31.2	31.2	31.2	15.6	15.6	31.2	31.2	31.3
	FOV (mm)	150	150	150	150	150	160	160	160
	Dimension	2D	2D	2D	2D	2D	3D	3D	3D
Differences (*p*-values) in the mean values between the direct measurements and the MRI measurements (mm)	Phantom 1 (Min width = 3.0 mm, m.d.e.m. = 9.94 mm)	0.45 **(p=0.05)**	0.48 **(p=0.02)**	0.48 **(p=0.03)**	0.35 (p=0.11)	0.61 **(p=0.007)**	0.40 **(p=0.05)**	0.39 (p=0.10)	0.41 (p=0.05)
	Phantom 2 (Min width = 2.5 mm, m.d.e.m. = 8.69 mm)	0.25 (p=0.22)	0.25 (p=0.56)	0.31 (p=0.29)	0.05 (p=0.47)	0.42 (p=0.35)	0.19 (p=0.35)	0.32 (p=0.14)	0.23 (p=0.12)
	Phantom 3 (Min width = 1.5 mm, m.d.e.m. = 6.38 mm)	0.042 (p=0.83)	0.33 (p=0.27)	0.06 (p=0.20)	-0.017 (p=0.40)	0.008 (p=0.76)	0.09 (p=0.74)	-0.050 (p=0.71)	0.07 (p=0.69)
	Phantom 4 (Min width = 0.5 mm, m.d.e.m. = 7.94 mm)	0.20 (p=0.51)	3.12 (p=0.22)	3.17 (p=0.21)	0.11 (p=0.45)	3.19 (p=0.20)	0.16 (p=0.63)	0.41 (p=0.20)	0.26 (p=0.34)

FOV field of view, *FSPGR* fast spoiled gradient-recalled echo, *GRE MPGR* multiplanar gradient-recalled echo, *Min full* minimum achievable TE with full echo acquisition, *m.d.e.m.* mean direct edge measurement, *Min width* minimum width, *N/A* not applicable, *NEX* number of excitations, *T1 SE* T1-weighted spin-echo, *TE* echo time, *TR* repetition time.

Statistical Analysis

Intra- and inter-reader reliabilities were examined by calculating differences between the repeated phantom edge measurements within and between readers. The mean and SD of these differences were used to address the issues of variability for the intra- and inter-reader phantom measurements. The intra- and inter-reader reliability for the measurements were assessed using coefficients of variations (CVs). The CVs were calculated as CV = (SD/mean) x 100% and expressed as a percentage to further assess the dispersion of data within and between the readers (18-20). CVs $\leqslant 10$ indicated an acceptable agreement between the readers in this study, based on previously published CVs from MRI-based measurements of knee cartilage volumes (21-26).

To determine whether the MRI-derived phantom measurements differed significantly from the direct phantom measurements (for different matrices and slice thicknesses), paired t-tests were performed. Bonferroni correction was used to adjust for multiple comparisons, with statistical significance set as alpha $\leqslant .007$ for all calculations. Borderline statistically significant differences were considered for *p*-values $> .007$ and $< .05$. All statistical analyses were performed using SAS, version 9.3 (SAS Institute, Cary, NC).

■ RESULTS

Direct Measurements *vs*. MRI-Derived Measurements

High inter-reader reliability was observed for both the direct phantom measurements, with CVs ranging from 2.50 to 6.40% (average, 4.40%) and for the MRI measurements, with CVs ranging from 0.61 to 7.75% (average, 3.15%). The intra-reader reliability was also high for both the direct and the MRI-derived measurements, with CVs ranging from 0.00 to 6.40% (average, 3.47%) and 0.00 to 6.49% (average, 1.64%), respectively.

Definite differences were noted between the mean direct measurements and the mean MRI-derived measurements for phantom 1 for the GRE MPGR sequence (512 x 512 pixels, 1.5-mm slice thickness, 5:49 min scan time; difference= 0.61 mm, *p*=.007). Borderline statistically significant differences were noted for the TI SE sequences with the following parameters: 320 x 320 pixels, 1.5-mm slice thickness, 6:11 min scan time (difference=0.45 mm, *p*=.049); 320 x 320 pixels, 4-mm slice thickness, 6:11 min scan time (difference=0.48 mm, *p*=.02); and 512 x 512 pixels, 1.5-mm slice thickness, 9:48 min scan time (difference=0.48 mm, *p*=.03). Borderline significant differences were also noted for the FSPGR sequence with 512 x 512 pixels, a 1.5-mm slice thickness, and a 3:36 min scan time (difference=0.40 mm, *p*=.048). No differences were noted between the mean direct measurements and the mean MRI-derived measurements (*p*-values > .05 for the different MRI sequences) for phantoms 2, 3 or 4 (Table 1).

Signal-to-Noise Ratio & Spatial Resolution

SNR values were calculated for all the MRI sequences under investigation (Table 2). The SNR values were sufficient and ranged from 8.60 to 90.7, with an average of 32.9. The spatial resolutions (gross assessment) of the MRI sequences were appropriate and ranged from 0.16 to 0.47 (Table 3).

■ DISCUSSION

The results of the current study show that FSPGR sequences, regardless of the combination of MRI parameters used and the thickness of the cartilage-mimicking structure under assessment, provide accurate measurements. Therefore, when considering feasibility from the perspective of scanning time, the 0.5-mm slice thickness, 512 x 512 pixel, 3:38 min scan appears to be the most appropriate sequence for imaging maturing cartilage. The 512 x 512 pixel, 1.5-mm slice thickness, 5:49 min GRE MPGR sequence and, to a
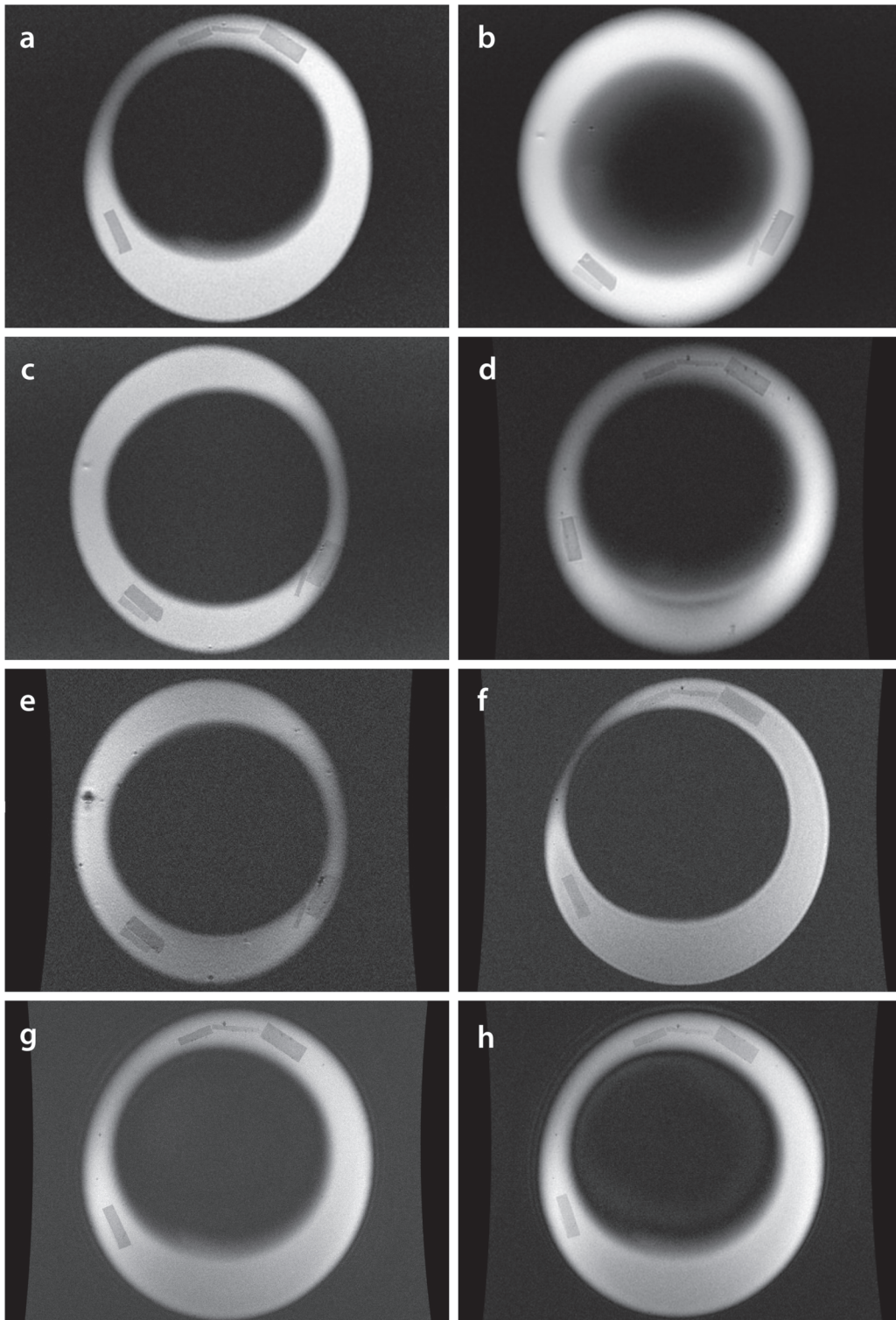
Figure 2 - Coronal MR images generated by various sequences and parameters.
(a) T1-weighted spin-echo (SE), 320 x 320 pixels, 1.5-mm slice thickness; (b) T1 SE, 320 x 320 pixels, 4-mm slice thickness; (c) T1 SE, 512 x 512 pixels, 1.5-mm slice thickness; (d) Multiplanar gradient-recalled echo (GRE MPGR), 320 x 320 pixels, 1.5-mm slice thickness; (e) GRE MPGR, 512 x 512 pixels, 1.5-mm slice thickness; (f) Fast spoiled gradient-recalled echo (FSPGR), 512 x 512 pixels, 0.5-mm slice thickness; (g) FSPGR, 1024 x 1024 pixels, 1.5-mm slice thickness; (h) FSPGR, 512 x 512 pixels, 1.5-mm slice thickness.

lesser degree, all the T1 SE sequences (regardless of the combination of parameters used) appeared suboptimal for producing accurate measurements of the phantom with the largest width.

To determine the accuracy of an MRI sequence in measuring pediatric articular cartilage, the paradigm of no statistically significant differences (and to a lesser extent no borderline differences) between the mean direct measurements and the mean MRI-derived measurements was taken into consideration, in addition to the SNRs, spatial resolutions and scan times for each given set of parameters.

Finally, it should be noted that the cartilage layers of a maturing skeleton have a similar thickness to the diameters of the phantoms used in this study (27).
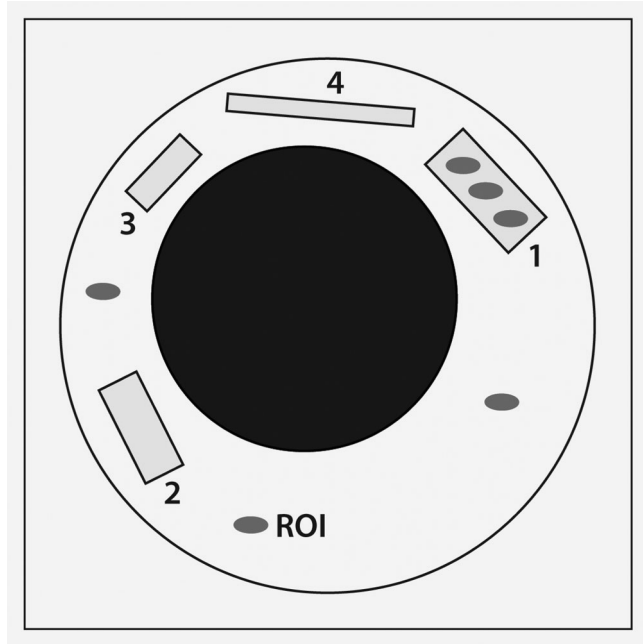
Phantom 1

Differences between the mean direct measurements and the mean MRI-derived measurements were only observed for phantom 1, the phantom with the largest width. This was the case for all MRI sequences (T1 SE, GRE MPGR and FSPGR) employed in this study, regardless of parameter variations. A possible explanation for this is the limitation imposed by the ruler used, which is only precise to 1 mm (± 0.5 mm). Therefore, any direct phantom edge measurement that fell between the 1-mm ruler increments was subjective. Given this fact, all the recorded measurements were rounded to the nearest 1-mm increment, resulting in a measurement error of ± 0.5 mm. Thus, we hypothesized that the widths of phantoms 2, 3 and 4 (3.8 mm, 2.1 mm and 1.3 mm, respectively) were too close to the measurement error of ± 0.5 mm to allow the readers to obtain accurate direct measurements. Therefore, because phantom 1 (largest width) was the only sample to provide accurate direct measurements of width, only this phantom was used to evaluate the accuracies of the MRI sequences in quantitatively maturing cartilage. The *p*-values, SNRs, spatial resolutions and scan times associated with phantom 1 are summarized in Table 3.

T1 SE

Despite adequate SNR and spatial resolution, the relatively long scan time (compared to the GRE MPGR and FSPGR sequences) and the borderline differences between the MRI-derived measurements and the reference standard measurements observed in this study led us to conclude that using a T1 SE sequence is inappropriate for accurately measuring pediatric articular cartilage in a clinical setting.

GRE MPGR

One of the two GRE MPGR sequences tested in this study (512 x 512 pixels, 1.5-mm slice thickness, 5:49 min scan time) appeared to be inappropriate for accurately measuring thin structures due to the significant differences observed between the MRI-derived measurements and the reference standard measurements. The SNR for this sequence was low (for all four phantoms) compared to all other sequences, with values ranging from 8.6 to 11.7 (average, 10). Therefore, noise may have contributed to poor image quality and thus less accurate MRI-derived measurements. Measurements from the other GRE MPGR sequence tested in this study (320 x 320 pixels, 4.0-mm slice thickness, 3:40 min scan time) demonstrated higher CVs and an overall better SNR than the above-referenced GRE MPGR sequence and could be performed

Figure 3 - Signal-to-noise ratio (SNR) calculation using MR images of phantoms 1-4 embedded in a saline bath. SNR was calculated as SNR=0.65*(signal intensity/standard deviation), employing a correction factor of 0.65 for background noise. The grey ovals represent 1-mm^2 regions of interest (ROIs).

faster (Table 3). However, this sequence had poorer spatial resolution (0.47 mm). GRE MPGR sequences are routinely used in clinical practice (28-30).

FSPGR

No significant differences were observed between the direct and MRI-derived measurements for any of the tested FSPGR sequences. Despite its good spatial resolution (0.16 mm), the FSPGR sequence using a 1024 x 1024 pixel resolution, 1.5-mm slice thickness and 10:33 min scan time appeared to be inappropriate for accurately measuring maturing cartilage given its low SNRs (range, 12.3-18.0; average, 15.1) and lengthy scan time. The other two FSPGR sequences, both using 512 x 512 pixel matrices, had comparable scan times and spatial resolutions (Table 3). However, the FSPGR sequence using a 512 x 512 pixel resolution, 0.5-mm slice thickness, and 3:36 min scan time had MRI measurements that were borderline statistically significantly different (*p*=.048) from the reference standard measurement for phantom 1.

Overall, according to this study, the FSPGR sequence using a 512 x 512 pixel matrix, 0.5-mm slice thickness and 3:38 min scan time appeared to be the most appropriate sequence for accurately measuring the dimensions of pediatric articular cartilage. This sequence had the second shortest scan time compared to the other sequences with similar parameters, making it desirable in a clinical setting. It also had an appropriate SNR and spatial resolution.

Almost two decades ago, a study was published showing that non-fat-suppressed and fat-suppressed fast low angle shot MRI (FLASH) sequences provided the most accurate determinations of the volume and thickness of adult

Table 2 - Signal-to-noise ratios for the magnetic resonance imaging sequences employed in this study.

		T1 SE			GRE MPGR			FSPGR	
Matrix (pixels)		320x320	320x320	512x512	320x320	512x512	512x512	512x512	1024x1024
Slice thickness (mm)		1.5	4	1.5	4	1.5	1.5	0.5	1.5
SNR	Phantom 1	44.4	66.5	25.8	35.0	11.7	39.2	21.7	15.4
	Phantom 2	38.2	79.8	31.0	44.9	8.6	47.6	22.4	18.0
	Phantom 3	27.0	90.7	34.1	19.2	10.0	31.9	21.1	12.3
	Phantom 4	33.6	84.9	33.5	23.7	9.7	36.8	20.7	14.5

FSPGR fast spoiled gradient-recalled echo, *GRE MPGR* multiplanar gradient-recalled echo, *SNR* signal-to-noise ratio, *T1 SE* T1-weighted spin-echo.

Table 3 - Summary of factors influencing the appropriateness of different MRI sequences for measuring maturing cartilage using phantom 1.

Pulse sequence	T1 SE			GRE MPGR			FSPGR	
Matrix (pixels)	320x320	320x320	512x512	320x320	512x512	512x512	512x512	1024x1024
Slice thickness (mm)	1.5	4	1.5	4	1.5	1.5	0.5	1.5
FOV (mm)	150	150	150	150	150	160	160	160
Scan time (min)	6:11	6:11	9:48	3:40	5:49	3:36	3:38	10:33
Spatial resolution (mm)	0.47	0.47	0.29	0.47	0.29	0.31	0.31	0.16
p-value	0.049	0.020	0.030	0.111	0.007	0.048	0.10	0.051
SNR	44.4	66.5	25.8	35.0	11.7	39.2	21.7	15.4

FOV field of view, *FSPGR* fast spoiled gradient-recalled echo, *GRE MPGR* multiplanar gradient-recalled echo, *SNR* signal-to-noise ratio, *T1 SE* T1-weighted spin-echo.

cartilage (10). More recent studies have confirmed this conclusion, stating that the use of FLASH at 1.5 T or 3 T remains the standard for quantifying articular cartilage (31-33). In recent years, double-echo steady-state imaging (DESS) with water excitation has gained interest as an alternate imaging modality for assessing cartilage due to its faster acquisition time and lower achievable slice thickness (34-38). However, it should be noted that DESS is still undergoing validation with regard to its ability to accurately measure cartilage dimensions (39). Other promising sequences for the assessment of cartilage include driven equilibrium Fourier transform (DEFT), which displays greater cartilage-to-fluid contrast than FLASH (40), balanced steady-state free precession (bSSFP) or true fast imaging with steady state (FISP) and its variant, fluctuating equilibrium magnetic resonance (FEMR) (41). Lastly, iterative decomposition of water and fat with echo asymmetry and least squares estimation (IDEAL) in combination with bSSFP demonstrates superior SNR, faster acquisition times and better contrast than FLASH (40). Again, it should be emphasized that quantitative cartilage data have not yet been presented with respect to any of the aforementioned sequences (DESS, DEFT, bSSFP/FISP, and IDEAL) (40). At the time of this writing, FLASH remains the MRI sequence of choice for accurately measuring the thickness and volume of maturing cartilage. This is concordant with the findings from the current study showing that FSPGR was the most appropriate sequence for accurately measuring pediatric cartilage-mimicking phantoms.

Study Limitations

One limitation of this study was the use of a steel ruler to obtain reference measurements. By using a "regression to the mean" approach (42), we expected to reduce human measurement error in this regard. We preferred to use "human eye" measurements as opposed to a contact-sensing dimension gage such as a micrometer because the mechanical perturbations associated with the use of a micrometer could have damaged the delicate phantoms used in this

study. In addition, we preferred to use paired t-test tests with Bonferroni corrections for multi-testing to compare the test and reference standard measurements rather than other methods that account for unequal variances such as Welch's method (43). The rationale for this was the fact that Welch's method is not suitable for paired comparisons and could over-correct the results in a pilot study with a restricted sample size. A limitation inherent in the use of paired t-tests was the assumption that the variances in the distributions of the test measurements and reference standard measurements were equal. As a consequence, one could argue that the results of this study could be unreliable if the variances between the underlying samples varied (43). Another limitation of the study was the fact that the same readers performed measurements of MR images and phantom specimens, which could have prompted recall bias. To avoid such bias, a time interval between reading sessions was established a priori. Finally, although the agar phantoms used in this study may not fully simulate the signal intensity or SNR of maturing cartilage on MRI, it would be extremely challenging to assess the signal intensities of layers of cartilage collected from cadavers of children for ethical reasons and results from animal cadavers would not represent the thickness of maturing cartilage in children.

In conclusion, based on scan time, reference standard comparability and accuracy, FSPGR proved to be the most optimal MRI sequence for measuring maturing cartilage-mimicking phantoms. Further translation of these results into the clinic should be performed to validate them and thus optimize the use of MRI sequences for the assessment of maturing cartilage in the pediatric population.

■ AUTHOR CONTRIBUTIONS

McKinney JR, Sussman MS, Amirabadi A, Rayner T and Doria AS conceived and designed the study. McKinney JR and Doria AS acquired, analyzed and interpreted the data. Moineddin R performed all statistical analyses of the data. McKinney JR drafted the manuscript. All authors critically reviewed the manuscript for important intellectual content and approved the final version for publication.

■ REFERENCES

1. Gougoutas AJ, Wheaton AJ, Borthakur A, Shapiro EM, Kneeland JB, Udupa JK, et al. Cartilage volume quantification via Live Wire segmentation. Acad Radiol. 2004;11(12):1389-95, http://dx.doi.org/10.1016/j.acra.2004.09.003.
2. Wang Y, Wluka AE, Jones G, Ding C, Cicuttini FM. Use magnetic resonance imaging to assess articular cartilage. Ther Adv Musculoskelet Dis. 2012;4(2):77-97, http://dx.doi.org/10.1177/1759720X11431005.
3. Hemke R, Doria AS, Tzaribachev N, Maas M, van der Heijde DM, van Rossum MA. Selecting magnetic resonance imaging (MRI) outcome measures for juvenile idiopathic arthritis (JIA) clinical trials: first report of the MRI in JIA special interest group. J Rheumatol. 2014;41(2):354-8, http://dx.doi.org/10.3899/jrheum.131081.
4. Miller E, Uleryk E, Doria AS. Evidence-based outcomes of studies addressing diagnostic accuracy of MRI of juvenile idiopathic arthritis. AJR Am J Roentgenol. 2009;192(5):1209-18, http://dx.doi.org/10.2214/AJR.08.2304.
5. Burgkart R, Glaser C, Hyhlik-Dürr A, Englmeier KH, Reiser M, Eckstein F. Magnetic resonance imaging-based assessment of cartilage loss in severe osteoarthritis: accuracy, precision, and diagnostic value. Arthritis Rheum. 2011;44(9):2072-7, http://dx.doi.org/10.1002/1529-0131(200109)44:9<2072::AID-ART357>3.0.CO;2-3.
6. Cicuttini F, Forbes A, Morris K, Darling S, Bailey M, Stuckey S. Gender differences in knee cartilage volume as measured by magnetic resonance imaging. Osteoarthritis Cartilage. 1999;7(3):265-71, http://dx.doi.org/10.1053/joca.1998.0200.
7. Peterfy CG, van Dijke CF, Janzen DL, Gluer CC, Namba R, Majumdar S, et al. Quantification of articular cartilage in the knee with pulsed saturation transfer subtraction and fat-suppressed MR imaging: optimization and validation. Radiology. 1994;192(2):485-91, http://dx.doi.org/10.1148/radiology.192.2.8029420.
8. Dupuy DE, Spillane RM, Rosol MS, Rosenthal DI, Palmer WE, Burke DW, et al. Quantification of articular cartilage in the knee with three-dimensional MR imaging. Acad Radiol. 1996;3(11):919-24, http://dx.doi.org/10.1016/S1076-6332(96)80299-6.
9. Eckstein F, Schnier M, Haubner M, Priebsch J, Glaser C, Englmeier KH, et al. Accuracy of cartilage volume and thickness measurements with magnetic resonance imaging. Clin Orthop Relat Res. 1998;(352):137-48.
10. Sittek H, Eckstein F, Gavazzeni A, Milz S, Kiefer B, Schulte E, et al. Assessment of normal patellar cartilage volume and thickness using MRI: an analysis of currently available pulse sequences. Skeletal Radiol. 1996;25(1):55-62, http://dx.doi.org/10.1007/s002560050032.
11. Graichen H, von Eisenhart-Rothe R, Vogl T, Englmeier KH, Eckstein F. Quantitative assessment of cartilage status in osteoarthritis by quantitative magnetic resonance imaging: technical validation for use in analysis of cartilage volume and further morphologic parameters. Arthritis Rheum. 2004;50(3):811-6, http://dx.doi.org/10.1002/art.20191.
12. Jones G, Ding C, Glisson M, Hynes K, Ma D, Cicuttini F. Knee articular cartilage development in children: a longitudinal study of the effect of sex, growth, body composition, and physical activity. Pediatr Res. 2003;54(2):230-6, http://dx.doi.org/10.1203/01.PDR.0000072781.93856.E6.
13. Spannow AH, Stenboeg E, Pfeiffer-Jensen M, Fiirgaard B, Haislund M, Ostergaard M, et al. Ultrasound and MRI measurements of joint cartilage in healthy children: a validation study. Ultraschall Med. 2001;32(Suppl 1):S110-6, http://dx.doi.org/10.1055/s-0029-1245374.
14. Rickey DW, Picot PA, Christopher DA, Fenster A. A wall-less vessel phantom for Doppler ultrasound studies. Ultrasound in Med Biol. 1995;21(9):1163-76, http://dx.doi.org/10.1016/0301-5629(95)00044-5.
15. McCann AJ, Workman A, McGrath C. A quick and robust method for measurement of signal-to-noise ratio in MRI. Phys Med Biol. 2013;58(11):3775-90, http://dx.doi.org/10.1088/0031-9155/58/11/3775.
16. Firbank MJ, Coulthard A, Harrison RM, Williams ED. A comparison of two methods for measuring the signal to noise ratio on MR images. Phys Med Biol. 1999;44(12):N261-4, http://dx.doi.org/10.1088/0031-9155/44/12/403.
17. Nitz WR, Balzer T, Grosu DS. Principles of magnetic resonance. In: Reimer P, Parizel PM, Meaney JFM, Stichnoth FA (eds). Clinical MR imaging: a practical approach. New York: Springer; 2010. p. 1-106.
18. Spannow AH, Pfeiffer-Jensen M, Andersen NT, Herlin T. Inter- and intra observer variation of ultrasonographic cartilage thickness assessments in small and large joints in healthy children. Pediatr Rheumatol. 2009;7:12, http://dx.doi.org/10.1186/1546-0096-7-12.
19. Eckstein F, Burstein D, Link TM. Quantitative MRI of cartilage and bone: degenerative changes in osteoarthritis. NMR Biomed. 2006;19(17):822-54, http://dx.doi.org/10.1002/nbm.1063.
20. Blumenkrantz G, Majumdar S. Quantitative magnetic resonance imaging of articular cartilage in osteoarthritis. Eur Cell Mater. 2007;13:76-86.
21. Jaremko JL, Cheng RW, Lambert RG, Habib AF, Ronsky JL. Reliability of an efficient MRI-based method for estimation of knee cartilage volume using surface registration. Osteoarthritis Cartilage. 2006;14(9):914-22, http://dx.doi.org/10.1016/j.joca.2006.03.004.
22. Eckstein F, Glaser C. Measuring cartilage morphology with quantitative magnetic resonance imaging. Semin Musculoskelet Radiol. 2004;8(4):329-53, http://dx.doi.org/10.1055/s-2004-861579.
23. Waterton JC, Solloway S, Foster JE, Keen MC, Gandy S, Middleton BJ, et al. Diurnal variation in the femoral articular cartilage of the knee in young adult humans. Magn Reson Med. 2000;43(1):126-32, http://dx.doi.org/10.1002/(SICI)1522-2594(200001)43:1<126::AID-MRM15>3.0.CO;2-#.
24. Heudorfer L, Hohe J, Faber S, Englmeier KH, Reiser M, Eckstein F. Precision MRI-based joint surface and cartilage density analysis of the knee joint using rapid water-excitation sequence and semi-automatic segmentation algorithm. Biomed Tech (Berl). 2000;45(11):304-10, http://dx.doi.org/10.1515/bmte.2000.45.11.304.
25. Glaser C, Burgkart R, Kutschera A, Englmeier KH, Reiser M, Eckstein F. Femoro-tibial cartilage metrics from coronal MR image data: technique, test-retest reproducibility, and findings in osteoarthritis. Magn Reson Med. 2003;50(6):1229-36, http://dx.doi.org/10.1002/mrm.10648.
26. Cicuttini FM, Wluka AE, Wang Y, Stuckey SL. Longitudinal study of changes in tibial and femoral cartilage in knee osteoarthritis. Arthritis Rheum. 2004;50(1):94-7, http://dx.doi.org/10.1002/art.11483.
27. Keshava SN, Gibikote SV, Mohanta A, Poonnoose P, Rayner T, Hillard P, et al. Ultrasound and magnetic resonance imaging of healthy paediatric ankles and knees: a baseline for comparison with haemophilic joints. Hemophilia. 2015;21(3):e210-22, http://dx.doi.org/10.1111/hae.12614.
28. Crema MD, Roemer FW, Marra MD, Burstein D, Gold GE, Eckstein F, et al. Articular cartilage in the knee: current MR imaging techniques and applications in clinical practice and research. Radiographics. 2011;31(1):37-62, http://dx.doi.org/10.1148/rg.311105084.
29. Laor T, Chung T, Hoffer FA, Jaramillo D. Musculoskeletal magnetic resonance imaging: how we do it. Pediatr Radiol. 1996;26(10):695-700, http://dx.doi.org/10.1007/BF01383382.
30. Greenspan P. Orthopedic imaging: a practical approach, 5th edn. Philadelphia: Lippincott Williams & Wilkins; 2011.
31. Eckstein F, Cicuttini F, Raynauld JP, Waterton JC, Peterfy C. Magnetic resonance imaging (MRI) of articular cartilage in knee osteoarthritis (OA): morphological assessment. Osteoarthritis Cartilage. 2006;14(Suppl A):A46-75, http://dx.doi.org/10.1016/j.joca.2006.02.026.
32. Gold GE, Burstein D, Dardzinski B, Lang P, Boada F, Mosher T. MRI of articular cartilage in OA: novel pulse sequences and compositional/functional markers. Osteoarthritis Cartilage. 2006;14(Suppl A):A76-86, http://dx.doi.org/10.1016/j.joca.2006.03.010.
33. Peterfy CG, Gold G, Eckstein F, Cicuttini F, Dardzinski B, Stevens R. MRI protocols for whole-organ assessment of the knee in osteoarthritis. Osteoarthritis Cartilage. 2006;14(Suppl A):A95-111, http://dx.doi.org/10.1016/j.joca.2006.02.029.
34. Eckstein F, Hudelmaier M, Wirth W, Kiefer B, Jackson R, Yu J, et al. Double echo steady state magnetic resonance imaging of knee articular cartilage at 3 Tesla: a pilot study for the Osteoarthritis Initiative. Ann Rheum Dis. 2006;65(4):433-41, http://dx.doi.org/10.1136/ard.2005.039370.
35. Wirth W, Nevitt M, Hellio Le Graverand MP, Benichou O, Dreher D, Davies RY, et al. Sensitivity to change of cartilage morphometry using coronal FLASH, sagittal DESS, and coronal MPR DESS protocols-comparative data from the Osteoarthritis Initiative (OAI). Osteoarthritis Cartilage. 2010;18(4):547-54, http://dx.doi.org/10.1016/j.joca.2009.12.003.
36. Hardy PA, Recht MP, Piraino D, Thomasson D. Optimization of a dual echo in the steady state (DESS) free-precession sequence for imaging cartilage. J Magn Reson Imaging. 1996;6(2):329-35, http://dx.doi.org/10.1002/jmri.1880060212.
37. Eckstein F, Kunz M, Hudelmaier M, Jackson R, Yu J, Eaton CB, et al. Impact of coil design on the contrast-to-noise ratio, precision, and consistency of quantitative cartilage morphometry at 3 Tesla: a pilot study for the osteoarthritis initiative. Magn Reson Med. 2007;57(2):448-54, http://dx.doi.org/10.1002/mrm.21146.
38. Eckstein F, Kunz M, Schutzer M, Hudelmaier M, Jackson RD, Yu J, et al. Two year longitudinal change and test-retest-precision of knee cartilage morphology in a pilot study for the osteoarthritis initiative. Osteoarthritis Cartilage. 2007;15(11):1326-32, http://dx.doi.org/10.1016/j.joca.2007.04.007.
39. Eckstein F, Wirth W. Quantitative cartilage imaging in knee osteoarthritis. Arthritis. 2011. Available from PubMed: http://www.ncbi.nlm.nih.gov/pubmed/22046518. http://dx.doi.org/10.1155/2011/475684.
40. Hargreaves BA, Gold GE, Lang PK, Conolly SM, Pauly JM, Bergman G, et al. MR imaging of articular cartilage using driven equilibrium.

Magn Reson Med. 1999;42(4):695-703, http://dx.doi.org/10.1002/(SICI) 1522-2594(199910)42:4<695::AID-MRM11>3.0.CO;2-Z.

41. Carballido J, Eckstein F. Quantitative morphological imaging of the knee joint. In: Majumdar S (ed) Advances in MRI of the knee for osteoarthritis. Singapore: World Scientific Publishing Co. Pte. Ltd.; 2010. p. 143-184.

42. Barnett AG, van der Pols JC, Dobson AJ. Regression to the mean: what it is and how to deal with it. Int J Epidemiol. 2005;34(1):215-20, http://dx.doi.org/10.1093/ije/dyh299.

43. Ruxton GD. The unequal variance t-test is an underused alternative to Student's t-test and the Mann–Whitney U test. Behav Ecol. 2006; 17(4):688-90, http://dx.doi.org/10.1093/beheco/ark016.